Electron trajectories in a free-electron laser with a reversed axial guide field

V. A. Bazylev
I. V. Kurchatov Institute of Atomic Energy, Moscow, Russia

A. Bourdier*
Commissariat à l'Energie Atomique, Centre d'Etudes de Bruyères-le-Châtel, 91680 Bruyères-le-Châtel, France

Ph. Gouard
Commissariat à l'Energie Atomique, Centre d'Etudes de Limeil-Valenton, 94195 Villeneuve-Saint-Georges Cedex, France

J. M. Buzzi
Laboratoire de Physique des Milieux Ionisés, Ecole Polytechnique, Centre National de la Recherche Scientifique, 91128 Palaiseau Cedex, France

(Received 3 May 1993)

In order to interpret an experiment of Conde and Bekefi [Phys. Rev. Lett. **67**, 3082 (1991); **68**, 418 (E) (1992)], electron trajectories are studied for a configuration with a reversed axial guide field. First, ignoring the radial dependence of the wiggler, an analytic model is constructed. The results are discussed and compared with those of numerical simulations. Close to "antiresonance," two types of electron trajectories are considered and discussed. One type corresponds to a linearly polarized motion and leads to a moderate coupling with the radiation field. This first part shows how electrons, which remain close to the axis of the beam, can contribute to the observed dip in the power output. Then the radial dependence of the wiggler is considered. In the vicinity of "antiresonance," electrons are shown to have "chaotic" trajectories when emitted far enough from the axis. As a consequence, the interaction efficiency is degraded for most particles. This explains the large dip in radiative power observed and predicted by our simulation computer code. The radial dependence also gives a possible explanation for the very good efficiency observed in the experiment.

PACS number(s): 41.60.Cr, 47.52.+j

I. INTRODUCTION

Recently, Conde and Bekefi [1] reported on a free-electron-laser (FEL) experiment using the reversed-field configuration, i.e., when the directions of $\mathbf{k}_\omega$ (the wave vector of the wiggler) and the guide field $\mathbf{B}_0$ are opposite. Significant new features in the character of the emission have been found compared to those in the direct-field configuration ($\mathbf{k}_\omega$ in the direction of $\mathbf{B}_0$). One is a high conversion efficiency. At "antiresonance," when the cyclotron wavelength is close to the wiggler period, a large dip in the radiation is observed. There has already been theoretical work, including numerical simulations [2,3], to explain these phenomena.

In Sec. II, neglecting the radial dependence of the wiggler, a steady-state analytic solution for the electron trajectories is derived. The fact that this solution is an appropriate one is shown with a three-dimensional nonlinear simulation computer code, SOLITUDE [4], and can also be shown with our trajectory code HÉLIX. This simple model permits us to predict, close to antiresonance, a small dip in the power output in the case of a thin-electron-beam experiment. It also shows how, in the experiment of Conde and Bekefi, electrons which remain close to the axis can contribute to create the dip observed in the radiation output. The contribution is significant only when the beam has some emittance combined with energy spread. This model is also convenient to explain simply the foundations of our method.

In Sec. III, the radial dependence of the wiggler is taken into account. On the one hand, we confirm that, close to antiresonance, the trajectories of electrons emitted far enough from the axis of the beam are "chaotic"; they undergo a very irregular axial motion [3]. The large variations in the axial momentum disrupt the resonant wave-particle interaction for most particles. On the other hand, a possible explanation is given for the good efficiency in the reversed-field configuration. SOLITUDE gives results in good agreement with the experiment.

II. ANALYTIC MODEL IGNORING THE RADIAL DEPENDENCE OF THE WIGGLER

The total magnetic field considered here is

$$\mathbf{B} = -B_0\mathbf{e}_z + B_\omega(\mathbf{e}_x \cos k_\omega z + \mathbf{e}_y \sin k_\omega z) , \tag{1}$$

where B_0 and B_ω are the amplitude of the axial guide and wiggler fields, respectively, and k_ω is the wiggler wave number.

We start with the Lorentz force equation for one electron leading to the following set of equations for the transverse velocity:

$$\frac{d}{dt}v_x=\omega_0 v_y+\alpha_\omega v_z \sin k_\omega z \ , \tag{2a}$$

$$\frac{d}{dt}v_y=-\omega_0 v_x-\alpha_\omega v_z \cos k_\omega z \ , \tag{2b}$$

where $\omega_0=eB_0/m\gamma$, γ is the Lorentz factor, and $\alpha_\omega=eB_\omega/m\gamma$.

For simplicity, z is taken as an independent variable. Introducing a complex velocity $v=v_x+iv_y$ and denoting the derivative with respect to z by a dot, the equation governing the transverse motion becomes

$$\dot{v}+i\frac{\omega_0}{v_z}v=-i\alpha_\omega \exp(ik_\omega z) \ . \tag{3}$$

The solution can be written

$$v=\exp\left[-i\int_0^z \frac{\omega_0}{v_z}dz'\right] \times\left[K+\int_0^z(-i\alpha_\omega)\exp\left[ik_\omega z'+i\int_0^{z'}\frac{\omega_0}{v_z}dz''\right]dz'\right] , \tag{4}$$

where K is a constant of integration, depending on the initial conditions of the electrons.

Assuming that γ^{-1} and $|v|/c$ are small quantities, we have

$$\frac{1}{v_z}=\frac{1}{v_\parallel}\left[1+\frac{|v|^2}{2v_\parallel c}\right] , \tag{5}$$

where $v_\parallel=c(1-1/2\gamma^2)$.

The solution of Eq. (3) is supposed to be of the form

$$v=v_0\exp\left[-i\frac{\omega_0^*}{v_\parallel}z\right]+b\exp(-ik_\omega z)+a\exp(ik_\omega z) , \tag{6}$$

where v_0, b, and a are real amplitudes. ω_0^* will be determined to obtain a consistent solution.

Equation (6) leads to the following form for the modulus of the transverse complex velocity, namely,

$$|v|^2=v_0^2+b^2+a^2+2\,\mathrm{Re}\left\{v_0 b\exp\left[i\left[\frac{\omega_0^*}{v_\parallel}-k_\omega\right]z\right]+v_0 a\exp\left[i\left[\frac{\omega_0^*}{v_\parallel}+k_\omega\right]z\right]+ba\exp(2ik_\omega z)\right\} . \tag{7}$$

Consequently, with the use of Eq. (5), we obtain, when supposing that we are close to antiresonance,

$$\exp\left[-i\int_0^z\frac{\omega_0}{v_z}dz\right]=\exp\left[-i\frac{\tilde{\omega}_0}{v_\parallel}z\right]\exp\left\{-i\frac{\omega_0}{v_\parallel c}\frac{v_0 a}{(\omega_0^*+k_\omega v_\parallel)}\sin\left[\left[\frac{\omega_0^*}{v_\parallel}+k_\omega\right]z\right]\right\}\exp\left[-i\frac{\omega_0}{2v_\parallel^2 c}\frac{ba}{k_\omega}\sin(2k_\omega z)\right] , \tag{8}$$

with

$$\tilde{\omega}_0=\omega_0\left[1+\frac{a^2+(b+v_0)^2}{2v_\parallel c}\right] . \tag{9}$$

Taking into account dominant terms only, Eq. (6) for v and Eq. (8) in Eq. (4) gives

$$v_0\exp\left[-i\frac{\omega_0^*}{v_\parallel}z\right]+b\exp(-ik_\omega z)+a\exp(ik_\omega z)=\left\{K-\frac{\alpha_\omega v_\parallel}{\tilde{\omega}_0-k_\omega v_\parallel}\epsilon_1-\frac{\alpha_\omega v_\parallel}{\tilde{\omega}_0-\omega_0^*}\epsilon_2+\frac{\alpha_\omega v_\parallel}{\tilde{\omega}_0+k_\omega v_\parallel}\right\}\times\exp\left[-i\frac{\tilde{\omega}_0}{v_\parallel}z\right]+\frac{\alpha_\omega v_\parallel}{\tilde{\omega}_0-\omega_0^*}\epsilon_2\exp\left[-i\frac{\omega_0^*}{v_\parallel}z\right]+\frac{\alpha_\omega v_\parallel}{\tilde{\omega}_0-k_\omega v_\parallel}\epsilon_1\exp(-ik_\omega z)-\frac{\alpha_\omega v_\parallel}{\tilde{\omega}_0+k_\omega v_\parallel}\exp(ik_\omega z) , \tag{10}$$

where $\epsilon_1=\frac{1}{4}\omega_0 ba/k_\omega v_\parallel^2 c$ and $\epsilon_2=\frac{1}{2}\omega_0 v_0 a/(\omega_0^*+k_\omega v_\parallel)v_\parallel c$. As a consequence,

$$\tilde{\omega}_0-\omega_0^*=\frac{\omega_0}{2(\omega_0^*+k_\omega v_\parallel)}\frac{a}{c}\alpha_\omega , \tag{11}$$

$$a=-\frac{\alpha_\omega v_\parallel}{k_\omega v_\parallel+\tilde{\omega}_0} , \tag{12}$$

$$\tilde{\omega}_0-k_\omega v_\parallel=\frac{\omega_0}{4k_\omega v_\parallel}\frac{a}{c}\alpha_\omega , \tag{13}$$

$$K=v_{(z=0)}=v_0+a+b \ . \tag{14}$$

Equation (11) gives the expression of ω_0^* as a function of the other parameters. Introducing the mismatch

$$\delta=\frac{\omega_0}{v_\parallel}-k_\omega , \tag{15}$$

close to antiresonance, Eq. (13) leads to the following expression for δ:

$$\delta = -\frac{\omega_0}{2v_\parallel^2 c}[2a^2+(b+v_0)^2] . \tag{16}$$

When $a = \pm(b+v_0)$, the motion of electrons is linearly polarized and only a moderate coupling with the electromagnetic wave can occur. This corresponds to the following value of $\delta \equiv \delta_1$:

$$\delta_1 = -\frac{3\omega_0}{2v_\parallel^2 c}a^2 . \tag{17}$$

Indeed, considering that δ is given by Eq. (17) and $K = 2a$ ($v_x = 2a$ and $v_y = 0$ at some point $z = 0$, where the amplitude of the wiggler is constant) in accordance with Eq. (14), a linearly polarized numerical solution is obtained with SOLITUDE, when no coupling between an electromagnetic and plasma wave is considered (Fig. 1).

For different values of the reversed axial guide field, considering the other parameters are those of Conde and Bekefi's experiment, a is calculated with the help of Eq. (12). We assume that we have $a = \pm(b+v_0)$ corresponding, respectively, to $K = 2a$ and $K = 0$, and we notice that there is only one point or a very small zone close to antiresonance for which the relation $\delta \approx \delta_1$ is valid. Moreover, it has been shown numerically that the amplitude of the transverse velocity does not vary very much close to this point. As a consequence, as shown in Figs. 2(a) and 2(b), there is a small dip in the output power close to antiresonance, when a weak electromagnetic wave and space charge are taken into consideration to initiate the simulation of the experiment. The space-charge field is expanded in terms of a superposition of the Gould-Trivelpiece modes [4,5]. The electron trajectories, the evolution of the TE_{11} mode, and the space-charge modes are calculated through a set of nonlinear coupled differential equations.

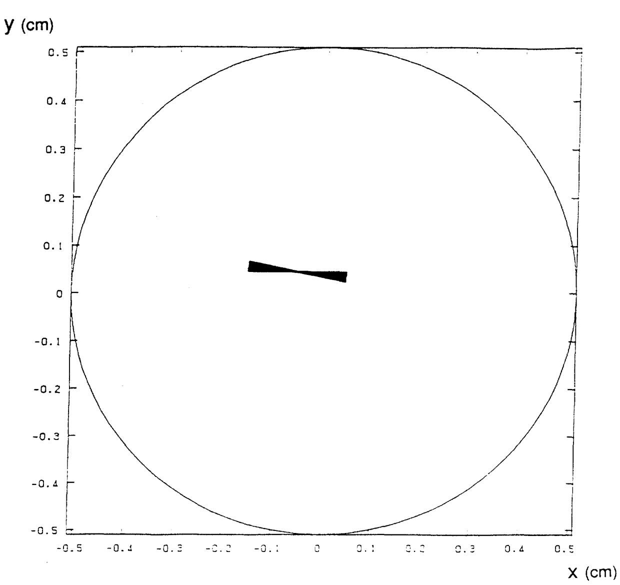

FIG. 1. Projection of an electron trajectory in the (x,y) plane for $K = 2a$ and $\delta = \delta_1$. The circle represents the waveguide wall in the case of Conde and Bekefi's experiment.

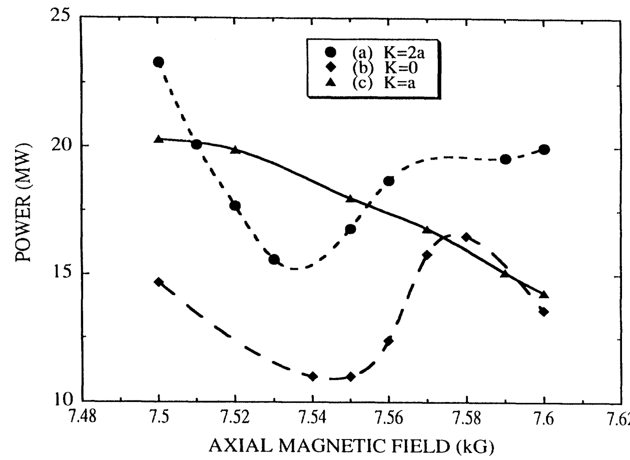

FIG. 2. FEL output power as a function of the axial field for (a) $K = 2a$, (b) $K = 0$, (c) $K = a$.

A circularly polarized motion for the electrons such as $b + v_0 = 0$ was also considered. Then, in the domain of validity of our analytic model, $\delta \equiv \delta_2$,

$$\delta_2 = -\frac{\omega_0}{v_\parallel^2 c}a^2 . \tag{18}$$

Simulations were performed taking $K = a$, that is, considering $v_x = a$, $v_y = 0$ at $z = 0$. Indeed, when $\delta = \delta_2$, we obtain a circularly polarized motion. It has been shown numerically that this situation corresponds to an electron trajectory at the end of the region where the amplitude of the wiggler increases adiabatically from zero to a constant level, when injected without emittance at the input. We have verified numerically that there is one point, close to antiresonance, such that $\delta = \delta_2$. Close to this point, the motion remains quasicircularly polarized and the perpendicular velocity varies gently. As displayed in

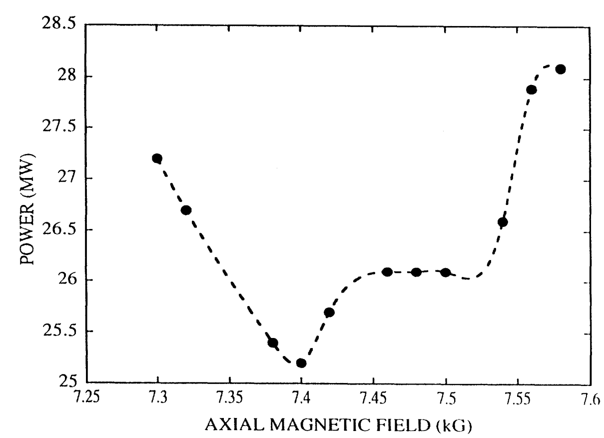

FIG. 3. The variation in the output power versus the magnitude of the reversed axial field obtained when the radial dependence of the wiggler is neglected, in the case of Conde and Bekefi's experiment.

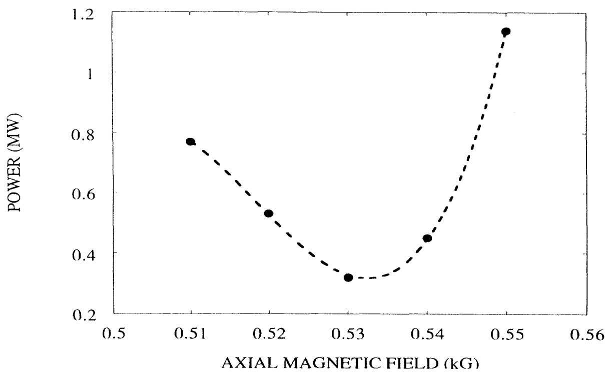

FIG. 4. The variation in the output power versus the magnitude of the reversed axial field when the radial dependence of the wiggler is neglected, in the case of a thin electron beam such as $k_\omega R_b = 0.1$.

Fig. 2(c), we found no dip close to it.

Figure 3 shows the variation in the output power versus the magnitude of the reversed axial field obtained with SOLITUDE without taking into consideration the radial dependence of the wiggler. The emittance and the energy spread of the beam are those of Conde and Bekefi's experiment ($\epsilon = 4.4\times10^{-4}$ m rad, the energy of the beam is $E_b = 750\pm50$ keV: $\Delta\gamma/\gamma = 0.04$).

Figure 4 displays the results of our simulations in the case of a thin electron beam, when the radial dependence can be ignored. The radius of the beam (R_b) is such that $k_\omega R_b \ll 1$. The situation considered corresponds to the Raman regime [6]. We assume that the wiggler field is produced by a bifilar helix with a period $\lambda_\omega = 12$ cm, a length of 3 m, and an adiabatic entry taper of 8 wiggler periods. The wiggler field magnitude is 0.147 T. The radius of the beam is 0.2 cm ($k_\omega R_b \approx 0.1$) and provides a wave beam coupling with a TE_{11} mode at a frequency of 96 GHz. The FEL is used as an amplifier. The electromagnetic mode is in the right-hand circular polarization with an initial power of 5×10^3 W. The emittance is the same as in Conde and Bekefi's experiment and the energy of the beam is centered on 2.5 MeV with a spread given by the condition $\Delta\gamma/\gamma = 0.01$.

III. ELECTRON TRAJECTORIES WHEN THE RADIAL DEPENDENCE OF THE WIGGLER IS CONSIDERED

In cylindrical coordinates (r,φ,z), the magnetic field components of the wiggler are represented by

$$B_{\omega r} = 2B_\omega I_1'(k_\omega r)\cos(\varphi - k_\omega z) ,$$
$$B_{\omega\varphi} = -2B_\omega \frac{I_1(k_\omega r)}{k_\omega r}\sin(\varphi - k_\omega z) , \quad (19)$$
$$B_{\omega z} = 2B_\omega I_1(k_\omega r)\sin(\varphi - k_\omega z) ,$$

where I_1 and I_1' denote the modified Bessel function of the first kind of order one and its derivative.

First, considering the case of the experiment of Conde and Bekefi, it has been verified that, in the vicinity of antiresonance, electrons initially located close to the edge of the beam have a chaotic motion [3]. Figure 5 shows the cross-sectional evolution of such a trajectory. Figure 6 shows the behavior of the corresponding axial momentum [7]. The trajectories are quite irregular as long as

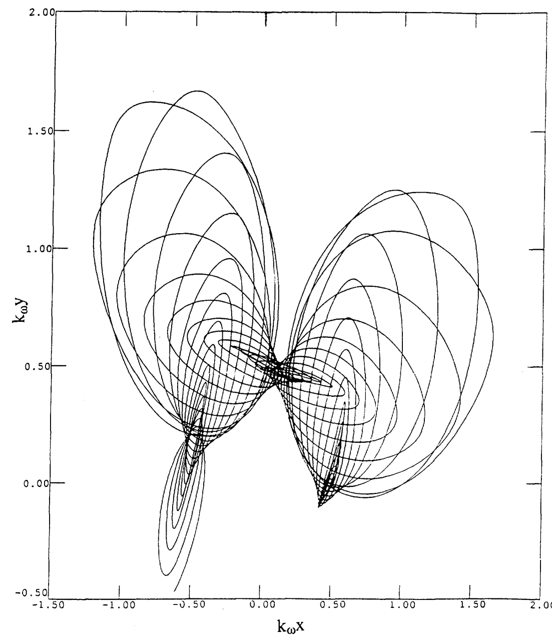

FIG. 5. The cross-sectional evolution of the trajectory of an electron injected at the edge of the beam for an axial field in the vicinity of antiresonance.

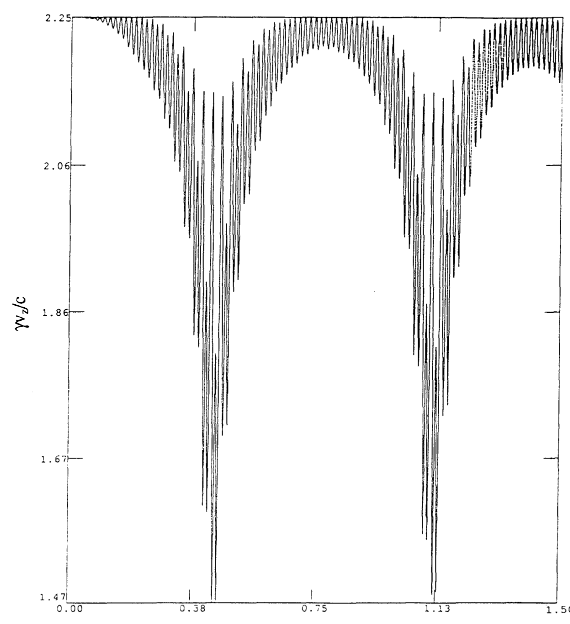

FIG. 6. The evolution of the axial momentum versus the axial position for the particle emitted at the edge of the beam in the neighborhood of antiresonance.

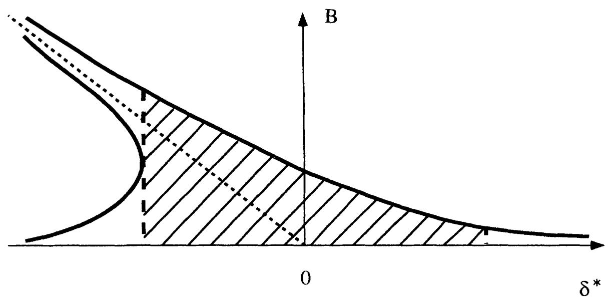

FIG. 7. The evolution of B vs the normalized mismatch δ^*.

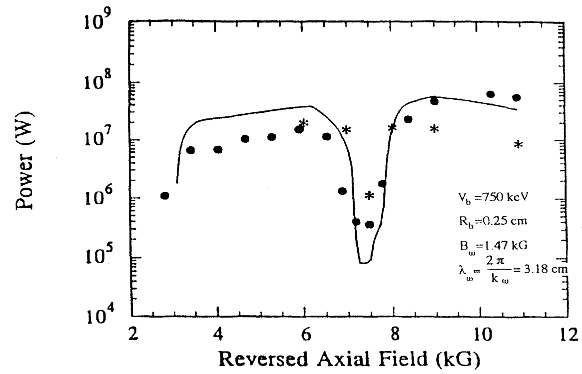

FIG. 8. The variation in the output power versus the magnitude of the reversed axial field as measured in the experiment (dots), with ARACHNE (solid curve), and with SOLITUDE (stars).

$k_\omega r_I \geq 0.2$ (where r_I is the initial distance of a particle from the axis of the beam). These rapid and large variations in the axial momentum affecting most particles seem to be the most important reason for the degradation of the wave-particle interactions at antiresonance and is the main reason for the large dip in power output observed in the experiment.

Now the influence of the particles, which are initially located not too far from the center of the beam when entering into the wiggler, is studied. We assume that $k_\omega r < 1$. The equation for the complex electron velocity can be derived just like in the preceding section, and is found to be of the form

$$\dot{v} + i\chi v = -iQ \ , \tag{20}$$

with

$$\chi = \frac{\omega_0}{v_z}\left[1 - 2\frac{\alpha_\omega}{\omega_0} I_1(k_\omega r)\sin(\varphi - k_\omega z)\right] \tag{21}$$

and

$$Q = \alpha_\omega [I_0(k_\omega r)\exp(ik_\omega z) + I_2(k_\omega r)\exp i(2\varphi - k_\omega z)] \ . \tag{22}$$

It is assumed that for most of the electrons of the beam one may write

$$r = r_0 + \Delta r \ , \quad \varphi = \varphi_0 + \Delta\varphi \ , \tag{23}$$

where $\Delta r / r_0 \ll 1$ and $\Delta\varphi / \varphi_0 \ll 1$.

Here again, the electron velocity is supposed to be described by the form defined by Eq. (6), in which a, b, and v_0 are complex numbers. This form is used in the solution of Eq. (20) to derive conditions similar to those given by Eqs. (11)–(14). Considering that the defect of resonance is not too important, that is,

$$N^{-1} < \frac{2\pi}{k_\omega}\delta \ll 1 \ , \tag{24}$$

where N is the number of wiggler periods, the following relation is obtained:

$$\delta^* = -\frac{Bc}{2v_\parallel} \pm 2\hat{a}\frac{I_2(k_\omega r_0)}{\sqrt{B}} \ , \tag{25}$$

with $B = \hat{b}^2$ and $\delta^* = \delta v_\parallel / \omega_0 + (c/2v_\parallel)(2\hat{a}^2 + \hat{v}_0^2)$. We have introduced for any quantity g, $\hat{g} = |g|/c$. Figure (7) shows the evolution of B vs δ^* according to Eq. (25).

The variation of the average longitudinal electron velocity versus the electron energy is given by

$$\frac{d}{d\gamma}\langle \hat{v}_z \rangle = \frac{1}{2}\frac{d}{d\gamma}(\gamma^{-2} + \hat{a}^2 + \hat{v}_0^2 + B) \ . \tag{26}$$

In the dashed area in Fig. 7, $\langle \hat{v}_z \rangle$ will change very quickly when there is a small change of the electron energy due to the emission of photons. This means that the wave-particle coupling rapidly deteriorates. It gives a possible explanation for the severe decrease in the output power in the neighborhood of the antiresonance. At the edge of the dashed area, when B goes to zero, $d\langle \hat{v}_z \rangle / d\gamma$ decreases, and the efficiency of the amplifier can be quite high in accordance with the experimental results.

Figure 8 shows the variation in the output power over an interaction length of 159 cm as a function of the magnitude of the reversed magnetic field predicted by SOLITUDE. The TE_{11} mode of the wave guide which is amplified has a frequency of 33.39 GHz and an initial power of 8.5 kW. Although no emittance and no energy spread are taken into account, a good agreement with the experimental results and previous simulations [3] (which did include an axial energy spread for the electrons of 1.5%) is obtained. If an emittance and energy spread had been taken into consideration in SOLITUDE a broader and deeper dip would have been obtained. The effect of emittance is to diminish the efficiency of the wave-particle coupling.

IV. CONCLUSIONS

It has been shown that, in the vicinity of the antiresonance, there is a weak coupling between the electrons and the radiation we want to amplify. First, an analytic model has been presented. This model is admittedly simple as the spatial dependence of the wiggler has been neglected.

It applies to electrons which have trajectories in a neighborhood of the axis. Those electrons can have a linearly polarized motion and they contribute to the dip in the power output when the beam has some emittance and some energy spread leading to many K values. When the radial dependence of the wiggler is taken into consideration, it has been shown that, very close to antiresonance, the wave-particle coupling is disrupted because of the rapid variation of the axial velocity. The electrons initially located far enough from the axis of the beam were shown to have a chaotic axial momentum. Most of the electrons of the beam are in such a state. This explains the large dip in power output observed in Conde and Bekefi's experiment.

Far enough from the antiresonance, the sensitivity of the axial velocity to any energy variation decreases. This is a possible explanation for the very good amplifier efficiency observed in the experiment.

ACKNOWLEDGMENTS

The authors wish to thank Professor H. Wilhelmsson and D. Gardent for very valuable discussions.

*Also at Laboratorie de Physique des Milieux Ionisés, Ecole Polytechnique, Centre National de la Recherche Scientifique, 91128 Palaiseau Cedex, France.

[1] M. E. Conde and G. Bekefi, Massachusetts Institute of Technology Report No. PFC/JA-91-9, 1991 (unpublished); Phys. Rev. Lett. **67**, 3082 (1991); **68**, 418(E) (1992).

[2] Xiao-jian Shu, Phys. Lett. A **162**, 274 (1992).

[3] H. P. Freund and A. K. Ganguly, IEEE Trans. Plasma Sci. **PS-20**, 245 (1992).

[4] J. Gardelle and Ph. Gouard, Commissariat à l'Energie Atomique Report No. C.E.A.-R-5617, 1992 (unpublished).

[5] N. A. Krall and A. W. Trivelpiece, *Principles of Plasma Physics* (McGraw-Hill, New York, 1973).

[6] J. M. Buzzi, in *High-Brightness Accelerators,* Vol. 178 of *NATO Advanced Study Institute, Series B: Physics,* edited by A. K. Hyder, M. F. Rose, and A. H. Guenter (Plenum, New York, 1988), p. 369.

[7] D. Gardent (private communication).